Available online at www.sciencedirect.com

ScienceDirect

Procedia Engineering 175 (2017) 124 – 132

Procedia Engineering

www.elsevier.com/locate/procedia

1st International Conference on the Material Point Method, MPM 2017

Modelling screwpile installation using the MPM

Lei Wang[a,*], William M. Coombs[a], Charles E. Augarde[a], Michael Brown[b], Jonathan Knappett[b], Andrew Brennan[b], David Richards[c], Anthony Blake[c]

[a]*Durham University, Stockton Rd, Durham DH1 3LE*
[b]*University of Dundee, Nethergate, Dundee DD1 4HN*
[c]*University of Southampton, Highfield, Southampton SO17 1BJ*

Abstract

Screwpiles are, as the name suggests, piled foundations which are screwed into the ground. They provide restraint to both upwards and downward loading directions and are commonly used for light structures subject to overturning or wind loading, such as sign gantries at the sides of motorways. An EPSRC-funded project led by University of Dundee has recently started, with Durham and Southampton as partners, in which the use of screwpiles (individual or in groups) for offshore foundations is under investigation. At Durham, a numerical modelling framework based on the material point method (MPM) is being developed for the installation phase of a screwpile. The aim is to use the model to provide an accurate representation of the *in situ* ground conditions once the pile is installed, as during installation the ground is disturbed and any model that "wishes in place" a screwpile may not provide representative long-term performance predictions. Following modelling of installation, the soil state will be transferred to a standard finite element package for the subsequent modelling of in-service performance (the MPM being considered unnecessary and computationally expensive for this phase of the life of a screwpile). In this preliminary work, we present the development of features of this numerical tool to simulate the screwpile installation. These features include a moving mesh concept (both translation and rotation) and interface elements. The effectiveness of the algorithm is illustrated through simple examples.

Peer-review under responsibility of the organizing committee of the 1st International Conference on the Material Point Method
Keywords: screwpile; penetration problem; implicit MPM; moving mesh; elasto-plastic interface element; implicit stress integration.

1. Introduction

Foundation selection plays an important role in the overall concept design for offshore wind farms as there are large financial implications attached to the choices made. Typically, foundation costs are 25 to 34% of the overall costs [1]. There are several types of substructures used for offshore wind farms, including monopiles, gravity bases and jacket structures. Among them, the monopile, as shown in Figure 1, is currently most widely used due to ease of installation. Recently, Byrne and Houlsby [2] proposed the use of helical piles as an innovative foundation design option for offshore wind turbines. Screw (or helical) piles (Figure 1) are foundations which are screwed into the ground. They are widely used onshore for supporting motorway signs and gantries as they possess good tensile *and* compressive

* Corresponding author.
E-mail address: lei.wang@durham.ac.uk

Peer-review under responsibility of the organizing committee of the 1st International Conference on the Material Point Method
doi:10.1016/j.proeng.2017.01.040

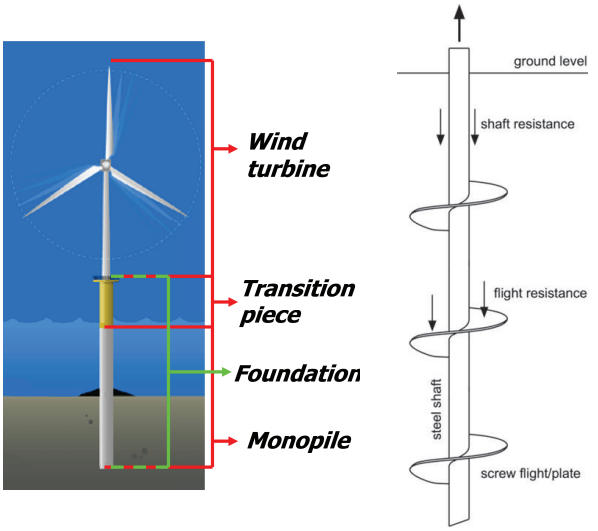

Fig. 1. Left: monopile foundation, a hollow cylindrical steel tube, currently widely used for wind turbine foundation. Right: The schematic of a screwpile.

resistance. The installation of a screwpile is generally cheaper, quicker and quieter, compared to conventional impact driving for monopiles.

An EPSRC-funded project which aims to explore the use of screwpiles as an alternative foundation option offshore for wind farms has recently begun, involving the universities of Dundee, Durham and Southampton. The UK has challenging targets for expansion of energy from renewables with the potential for over 5000 offshore wind turbines by 2020. The necessary move to deeper water will increase cost and put greater demands on subsea structures and foundations. To meet offshore demands, screwpiles will require geometry enhancement but it is envisaged that these will initially be modest to allow de-risked transfer of onshore technology offshore [3].

At Durham, the focus is on developing numerical models to aid this optimization. In particular, a numerical modelling framework based on the *implicit Material Point Method (MPM)* is being developed for the installation phase of a screwpile. The implicit MPM has advantages in accuracy over the earlier, simpler, explicit MPM, e.g. [4–6]. Our aim is to use the method to provide an accurate prediction of the *in situ* ground condition once the pile is installed, as during installation the ground is disturbed significantly and any model that "wishes in place" a screwpile may not provide representative predictions when the pile is subjected to in-service loads [7]. Following installation, the ground model is to be transferred to a standard finite element package for the subsequent modelling of in-service effects (the MPM being considered unnecessary and computationally expensive for this phase of the life of the screwpile). In this paper we present some preliminary development work of this installation model which makes use of a *moving mesh concept*, as in [8,9], and an elasto-plastic interface element for pile-soil interaction. Here we extend the moving mesh concept to include rotation as well as translation, both of which are required when installing a screwpile. The elasto-plastic interface constitutive law is implemented using an implicit stress integration approach, and the consistent tangent stiffness matrix is derived to significantly enhance the convergence rate of the Newton-Raphson solver for the equilibrium equations [10].

2. Methodology

2.1. Material Point Method

The MPM is very similar to the finite element method (FEM) but overcomes problems associated with mesh distortion, so it is ideally suited to model large deformation problems, such as soil-structure interaction in pile installation

and seabed ploughing [11]. In the MPM, a body is discretised using material points, and all spatial and temporal variables are held on these points (such as displacement, stress, history parameters, etc.). An arbitrary computational background mesh is used to solve the equilibrium equations. In the original MPM, standard FE basis functions are used to map between these two systems. Several extensions have been proposed to the original MPM that reduce cell-crossing instabilities, however for simplicity in this paper we use the original MPM. A typical calculation step in the MPM includes three phases (as shown in Figure 2): (i) the information held on material points is mapped to the background mesh nodes, (ii) the equilibrium equations are solved on the background mesh to obtain the displacement of the mesh nodes, and the nodal displacements are mapped to the material points and (iii) the FE mesh is replaced with a new mesh (typically the same as the original mesh).

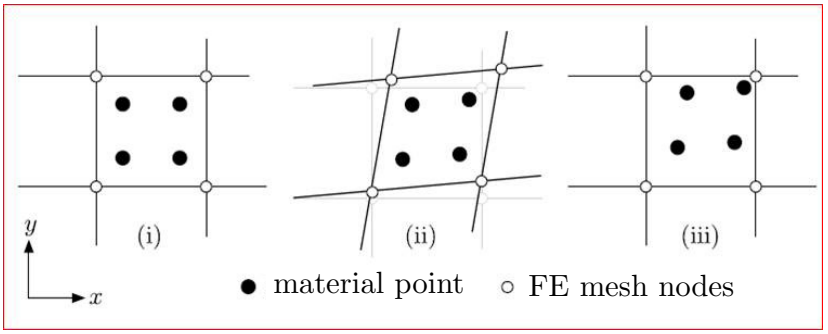

Fig. 2. The three phases in one computational step of the material point method: (i) the information held on material points is mapped to the background mesh nodes, (ii) the equilibrium is solved on the mesh to obtain the displacement of the mesh nodes, and (iii) the mesh is reset; after [12].

2.2. Moving mesh concept

The *moving mesh concept* can be simply thought as using a mesh that coincides with the boundary of a moving body (such as a pile penetrating into a soil domain). This allows easy specification of boundary conditions. However the movement of the mesh is decoupled from the movement of the material points. The displacement of the boundary is imposed in the same way as for conventional finite element analysis and all other physical displacements are solved via the equilibrium equations. Once these have been obtained they are mapped to the material points and then the mesh translated to remain coincident with the boundary of the moving body.

Assuming that the pile is a rigid body, during the installation of a screwpile the location of the soil-pile interface is known. The installation of a screwpile includes two kinds of movement: translation and rotation. Here we extend the moving mesh concept to include both translation and rotation; all previous approaches have only specified translation. The following section describes the algorithm for updating the mesh and, for the sake of clear demonstration, follows the concept through simplified 2D examples. The steps required to extend these algorithms to 3D should be self-evident.

2.2.1. Translating mesh

Consider a square body stretched along the vertical direction in Figure 3. In the undeformed configuration, the boundary of the body coincides with edges of the background mesh. Applying the moving mesh concept, the mesh in red is stretched and the mesh in blue is compressed, such that the boundary of the body always coincides with the edges of the background mesh. In this simple example the coordinates of nodes in the red mesh in this region are updated through

$$y \Leftarrow \frac{L_b + u}{L_b} y, \tag{1}$$

where y is the second component of a nodal coordinate with $y = 0$ at bottom, and u is the displacement applied to the top of the stretched body. At the same time, the mesh in blue is compressed. That is, coordinates of nodes in this

region are updated as

$$y \Leftarrow L_m - \frac{(L_m - L_b - u)(L_m - y)}{L_m - L_b}. \tag{2}$$

The top of the body is also updated, i.e. $L_b \Leftarrow L_b + u$. The condition for selecting nodes in the red mesh is $0 \leqslant y \leqslant L_b$, and the condition for nodes in the blue mesh is $y > L_b$.

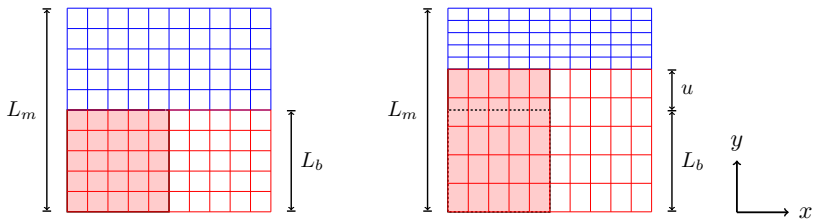

(a) undeformed configuration (b) deformed configuration

Fig. 3. The pink body is stretched by u along the vertical direction. The vertical length of the mesh is L_m, and of the body is L_b. The red mesh is stretched and the blue mesh is compressed, such that the boundary of body coincides with the edges of mesh.

2.2.2. *Rotating mesh*

Consider a circular region with an elliptical hole at the centre, as shown in Figure 4. The outer circle is fixed and a rotational boundary condition is applied to the ellipse. The mesh is rotated by the same amount on the ellipse, such that the ellipse always conforms with the boundary. Consistent with the incremental rotation degree, $\Delta\theta$, the mesh nodal coordinates are updated as

$$x_1 \Leftarrow x_0 \cos(\Delta\theta) + y_0 \sin(\Delta\theta), \tag{3}$$

$$y_1 \Leftarrow -x_0 \sin(\Delta\theta) + y_0 \cos(\Delta\theta), \tag{4}$$

where (x_0, y_0) are the nodal coordinates at the beginning of the incremental loading step and (x_1, y_1) are the updated nodal coordinates at the end of incremental loading step.

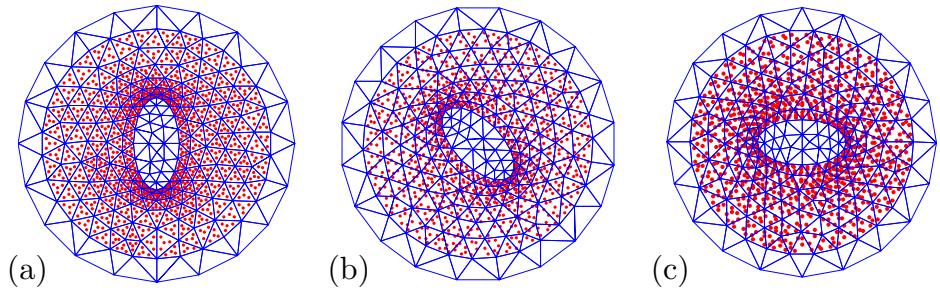

Fig. 4. (a) The initial computational mesh and material points, (b) and (c) are material points distribution subject to a twist 45° and 90°. The mesh is also rotated by 45° and 90° in (b) and (c), respectively.

2.3. *Elastic interface element*

A straightforward approach to modelling the interaction between the pile and the soil is to use interface elements that cover the surface of the pile. Unlike constitutive equations for continuum elements (working in terms of stress and strain), the constitutive law for this interface element is given by a traction vector against relative displacement between two faces of the interface element. In this section we introduce this relative displacement and traction vector for this interface element [13].

Relative displacement

For a two dimensional problem, a four-node zero-thickness interface element is considered, as shown in Figure 5. 1–2 and 4–3 are straight lines and the pairs of nodes (1,4) and (2,3) are each coincident before deformation. Let $\boldsymbol{u}_n = [u_1 \ v_1 \ u_2 \ v_2 \ u_3 \ v_3 \ u_4 \ v_4]^T$ denote the nodal displacements. Displacements along the lines 1–2 and 4–3 can be approximated by using linear interpolation functions in terms of a local coordinate $-1 \leqslant \xi \leqslant 1$

$$N_1(\xi) = \frac{1}{2}(1-\xi), \qquad N_2(\xi) = \frac{1}{2}(1+\xi), \tag{5}$$

that is, the relative displacement between nodes 1 and 2 is

$$\boldsymbol{u}_{12} = \begin{bmatrix} N_1 & 0 & N_2 & 0 & 0 & 0 & 0 & 0 \\ 0 & N_1 & 0 & N_2 & 0 & 0 & 0 & 0 \end{bmatrix} \boldsymbol{u}_n, \tag{6}$$

and between nodes 3 and 4

$$\boldsymbol{u}_{43} = \begin{bmatrix} 0 & 0 & 0 & 0 & N_2 & 0 & N_1 & 0 \\ 0 & 0 & 0 & 0 & 0 & N_2 & 0 & N_1 \end{bmatrix} \boldsymbol{u}_n. \tag{7}$$

The relative displacement at a point between the line 1–2 and 4–3 is

$$\boldsymbol{w} = \boldsymbol{u}_{43} - \boldsymbol{u}_{12} = \mathbf{B}\boldsymbol{u}_n, \tag{8}$$

where

$$\mathbf{B} = \begin{bmatrix} -N_1 & 0 & -N_2 & 0 & N_2 & 0 & N_1 & 0 \\ 0 & -N_1 & 0 & -N_2 & 0 & N_2 & 0 & N_1 \end{bmatrix}. \tag{9}$$

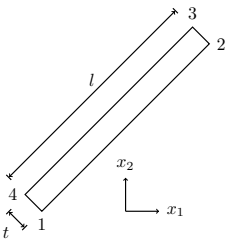

Fig. 5. Four-node zero-thickness element, with thickness $t = 0$ and length l.

Constitutive law

An elastic constitutive law for the interface element can be expressed as

$$\boldsymbol{\sigma} = \mathbf{D}\boldsymbol{w}, \tag{10}$$

where the traction vector and stiffness matrix are respectively

$$\boldsymbol{\sigma} = [\sigma_s \ \ \sigma_n]^T \qquad \text{and} \qquad \mathbf{D} = \begin{bmatrix} k_s & 0 \\ 0 & k_n \end{bmatrix}.$$

where k_s and k_n are the shear and normal stiffness of the interface. Assigning a large value for both k_s and k_n results in a no-slip condition at the interface, whereas assigning a very small value to k_s allows the interface to model sliding.

2.4. Elasto-plastic interface element

To model the *large* sliding expected between the pile and the soil, an elasto-plastic interface element is required. An elastic-plastic constitutive law for interface elements can be expressed in rate form as

$$\dot{\boldsymbol{\sigma}} = \mathbf{D}(\dot{\boldsymbol{w}} - \dot{\boldsymbol{w}}^p), \tag{11}$$

where $\boldsymbol{w}^p$ denotes the irreversible slip between two faces. The irreversible relative displacement $\boldsymbol{w}^p$ is determined by the Mohr-Coulomb constitutive law. This law consists of a yield function $f(\boldsymbol{\sigma})$ and a plastic potential $g(\boldsymbol{\sigma})$. They are

$$f(\boldsymbol{\sigma}) = |\sigma_s| + \sigma_n \tan\phi - c = 0 \tag{12}$$

$$g(\boldsymbol{\sigma}) = |\sigma_s| + \sigma_n \tan\psi = 0, \tag{13}$$

where σ_s is the shear stress and σ_n is the normal stress; c, ϕ and ψ are the cohesion, angle of friction and angle of dilation, respectively. The irreversible slip rate $\dot{\boldsymbol{w}}^p$ is determined by

$$\dot{\boldsymbol{w}}^p = \dot{\lambda}\frac{\partial g}{\partial \boldsymbol{\sigma}}, \tag{14}$$

where $\frac{\partial g}{\partial \boldsymbol{\sigma}}$ determines the direction of plastic slip and $\dot{\lambda}$ is the magnitude of the plastic slip rate. The time integration of this constitutive equation is performed using the backward Euler implicit method. In addition, this implementation employs an algorithmic consistent tangent for the global equilibrium solution. This tangent provides the linearisation of the constitutive equations as a function of the trial elastic strain. The use of this consistent tangent within the global equilibrium iterations allows for asymptotic quadratic convergence to zero of the residual out-of-balance force, leading to optimum efficiency of the Newton-Raphson solver [10].

3. Numerical simulations

In this section some numerical results are presented that demonstrate the procedures described in the previous section. The first example illustrates the application of a translating mesh in a plane strain 2D pile installation problem. As shown in Figure 6, a linear triangular mesh is used and initial material points are generated at the location of the Gauss quadrature points for the elements (with four points per element in the initial configuration). Due to symmetry only half of the problem is modelled and the pile is assumed to be a rigid body during installation. The black region shows the pile of width 1 m, which is initially inserted into the ground. For the sake of this demonstration, the soil is assumed to be an elastic isotropic material with Young's modulus, $E = 10$ kPa and Poisson's ratio, $\nu = 0$. The no-slip constraint is used at the interface between pile and soil. A displacement boundary condition is applied at the top of pile to drive the installation, i.e. at each loading step, a displacement of 0.1 m is applied. After 40 loading steps, the profile shown in Figure 6 is obtained. Due to the no-slip condition the material points are dragged downwards with the pile, resulting in an unrealistic deformed soil profile, i.e., the excessive deformation of the soil surface in the vicinity of the pile.

The second example demonstrates the rotating mesh concept. As shown in Figure 7, a circular region with an elliptical hole at the centre is modelled, and linear triangular elements are used to discretise the initial geometry with four material points per element in the original configuration. Additional elements are employed outside the physical domain in case the material points move unexpectedly (this was not the case in this simulation, however). The outer edge of the circular domain is fixed and a rotation boundary condition applied on the inner ellipse. In each incremental loading step, the rotation increment is 5°. The horizontal displacements of material points are plotted in Figure 7 for the cases of 45° and 90° rotation of the ellipse.

To illustrate the consequence of including an interface element between the soil and a translating rigid body, we initially use a purely elastic interface element. Assigning a small value for the tangential stiffness, k_s, allows the interface to model sliding. In this example $k_n = 10^5$ kPa was used to avoid the appearance of an unrealistic normal gap at the interface. Two cases are presented: $k_s = 10^4$ kPa for the "large k_s" case and $k_s = 10^{-2}$ kPa for the "small k_s" case in Figure 8. The Young's modulus of the soil, $E = 10$ kPa and Poisson's ratio, $\nu = 0$ as before. The two soil profiles are as expected, with the small k_s allowing sliding at the soil-pile interface.

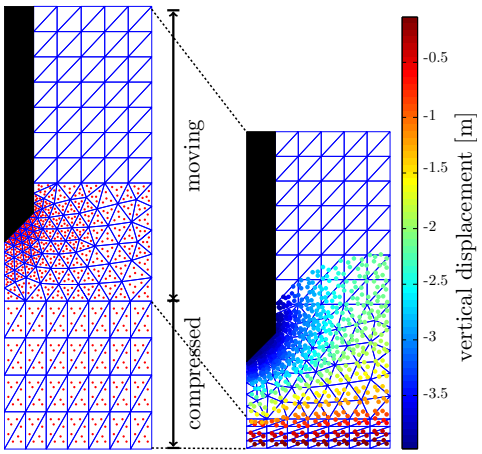

Fig. 6. 2D simulation of pile installation with no-slip condition on the soil-pile interface. The left is the mesh and material points in the initial configuration, while the right is the deformed configuration. The colourbar shows vertical displacement of the material points. The width of soil is 5 m and height is 15 m. The width of pile is 1 m and height is 8 m.

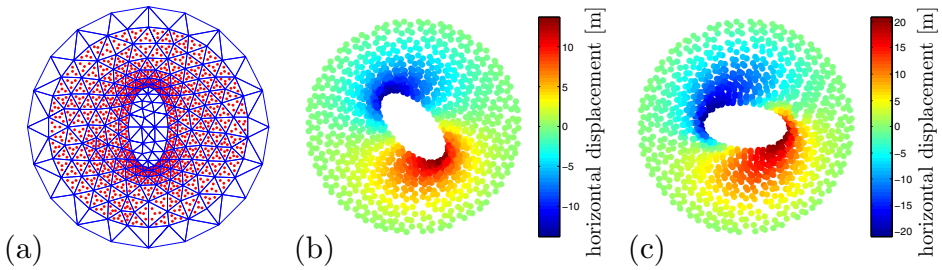

Fig. 7. (a) The mesh and material points in the initial configuration, (b) and (c) are material points distribution subject to twist 45° and 90°. Colours in (b) and (c) show the horizontal displacement.

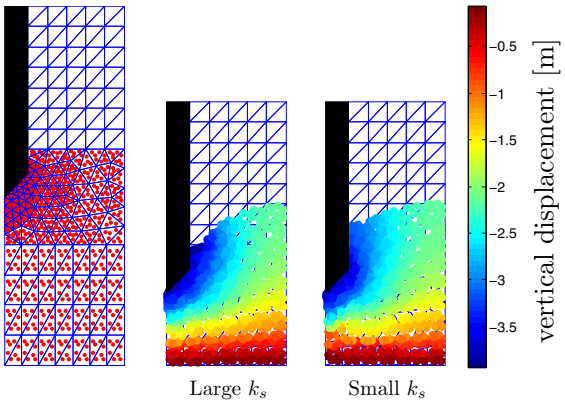

Fig. 8. With small k_s the top surface of soil after pile installation is more flat than with large k_s as expected.

For the elasto-plastic interface element, we demonstrate its effectiveness in the simple example shown in Figure 9 where two elastic continuum elements are used, joined by a single interface element. For the continuum element,

the Young's modulus, $E = 10\,\text{kPa}$, and Poisson's ratio, $\nu = 0$. For the interface element, $k_s = 10^4\,\text{kPa}$, $k_n = 10^4\,\text{kPa}$, $c = 10^{-4}\,\text{kPa}$, $\phi = 24°$ and $\psi = 0°$. Subject to a horizontal displacement of 0.5 m on the top nodes through 10 loading steps, the reaction force obtained is shown in Figure 9, demonstrating the elasto-plastic behaviour of the interface element and the large scale sliding between the two continuum elements.

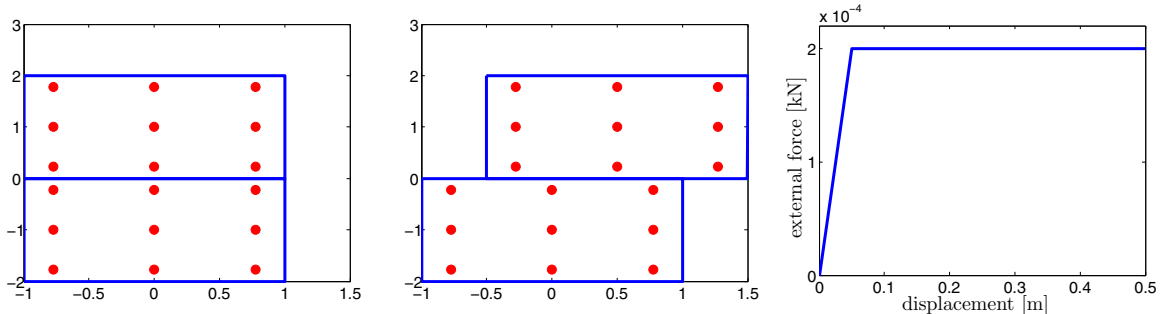

(a) initial configuration (b) deformed configuration (c) reaction force

Fig. 9. Elasto-plastic interface element: (a) initial configuration, (b) deformed configuration and (c) reaction force versus displacement.

4. Conclusion

This preliminary work develops a computational model based on the implicit MPM to simulate the installation of a screwpile. The moving mesh concept has been extended to allow rotation, which is essential when simulating screwpile installation. Through simplified 2D examples, the procedure has been illustrated, and extending these algorithms into a 3D simulation is straightforward. Both elastic and elasto-plastic interface elements have been implemented into the MPM code that allow the modelling of large slip soil-structural interaction. For the elasto-plastic interface element, a Mohr-Coulomb constitutive law with non-associated flow has been adopted. The implementation of this constitutive law uses implicit stress integration with a consistent algorithmic tangent to improve the accuracy of the solution and the efficiency of computation. In the future all the techniques will be combined into a 3D model for installation of a screwpile.

Acknowledgements

We are grateful for the support by the UK Engineering and Physical Sciences Research Council grant (No. EP/N006054/1).

References

[1] S. Bhattacharya, Challenges in design of foundations for offshore wind turbines, Engineering & Technology Reference(2014), 1-9, http://dx.doi.org/10.1049/etr.2014.0041.

[2] B. Byrne, G. Houlsby, Helical piles: an innovative foundation design option for offshore wind turbines, Philosophical Transactions of the Royal Society A 373 (2035) (2015) 20140081.

[3] J.A. Knappett, M.J. Brown, A.J. Brennan, L. Hamilton, Optimising the compressive behaviour of screw piles in sand for marine renewable energy applications. Int. Conf. On Piling & Deep Foundations, Stockholm, Sweden, 21st-23rd May 2014.

[4] J. E. Guilkey, J. A. Weiss, Implicit time integration for the material point method: Quantitative and algorithmic comparisons with the finite element method, International Journal for Numerical Methods in Engineering 57 (9) (2003) 1323–1338.

[5] D. Sulsky, A. Kaul, Implicit dynamics in the material-point method, Computer Methods in Applied Mechanics and Engineering 193 (12) (2004) 1137–1170.

[6] B. Wang, P. J. Vardon, M. A. Hicks, Z. Chen, Development of an implicit material point method for geotechnical applications, Computers and Geotechnics 71 (2016) 159–167.

[7] N. Phuong, A. van Tol, A. Elkadi, A. Rohe, Modelling of pile installation using the material point method (MPM), Numerical Methods in Geotechnical Engineering (2014) 271.
[8] L. Beuth, Formulation and application of a quasi-static material point method, University Stuttgart(2012).
[9] F. Ceccato, L. Beuth, P. A. Vermeer, P. Simonini, Two-phase material point method applied to the study of cone penetration, Computers and Geotechnics, In press.
[10] W. Coombs, Finite deformation of particulate geomaterials: frictional and anisotropic critical state elasto-plasticity, Ph.D. thesis, Durham University (2011).
[11] K. Lauder, M.J. Brown, M.F. Bransby, S. Boyes, The influence of incorporating a forecutter on the performance of off shore pipeline ploughs, Applied Ocean Research Journal (2013) 121130.
[12] M. Cortis, W.M. Coombs, C.E. Augarde, Implicit essential boundaries in the Material Point Method. Proceedings of the 24th UK Conference of the Association of Computational Mechanics in Engineering, Cardiff, UK, 31st Mar-1st Apr 2016.
[13] C.L. Ngo-Tran, The analysis of offshore foundations subjected to combined loading, Ph.D. thesis, University of Oxford (1996).